

# Mixed quark-nucleon phase in neutron stars and nuclear symmetry energy

M. Kutschera<sup>1,2</sup> and J. Niemiec<sup>1</sup>

<sup>1</sup> *H. Niewodniczański Institute of Nuclear Physics, ul. Radzikowskiego 152, 31-342 Kraków, Poland*

<sup>2</sup> *Institute of Physics, Jagiellonian University, ul. Reymonta 4, 30-059 Kraków, Poland*

(November 18, 2018)

The influence of the nuclear symmetry energy on the formation of a mixed quark-nucleon phase in neutron star cores is studied. We use simple parametrizations of the nuclear matter equation of state, and the bag model for the quark phase. The behavior of nucleon matter isobars, which is responsible for the existence of the mixed phase, is investigated. The role of the nuclear symmetry energy changes with the value of the bag constant  $B$ . For lower values of  $B$  the properties of the mixed phase do not depend strongly on the symmetry energy. For larger  $B$  we find that a critical pressure for the first quark droplets to form in the nucleon medium is strongly dependent on the nuclear symmetry energy, but the pressure at which last nucleons disappear is independent of it. We study the implications of these results for the structure of neutron stars. The finite-size effects are also considered. We find that the allowed range of surface tension for the mixed phase to be energetically favorable depends strongly on the nuclear symmetry energy.

PACS number(s): 26.60.+c, 21.65.+f, 97.60.Jd, 12.38.Mh

## I. INTRODUCTION

Recently, Glendenning [1] has shown that a proper construction of the nucleon-quark phase transition inside neutron stars implies the coexistence of nucleon matter and quark matter over a finite range of pressure. This has the effect that a core, or a spherical shell, of a mixed quark-nucleon phase can exist inside neutron stars. The fraction of space occupied by quark matter smoothly increases from zero at the core boundary, which corresponds to a critical pressure for the first quark droplets to form in the neutron star matter, to unity when eventually the last nucleons dissolve into quarks. Heiselberg *et al.* [2] included surface and Coulomb effects also in the mixed phase construction and concluded that the mixed phase remains the ground state of the neutron star matter for a physically reasonable range of surface tension.

In the original construction due to Glendenning, nucleon matter was treated in the relativistic mean field (RMF) model. The nuclear symmetry energy in the RMF model increases monotonically with the baryon number density [3]. This is in contrast to several variational many-body (VMB) calculations of the equation of state (EOS) of nuclear matter [4], which predict the symmetry energy to saturate and then to decrease at high densities. The aim of this paper is to study how sensitive the formation of a mixed quark-nucleon phase in neutron stars is to the high density behavior of the nuclear symmetry energy.

It was suggested in Ref. [1] that the isospin properties of the RMF model are responsible for the existence of the mixed quark-nucleon phase. We show here that it is the behavior of nucleon matter isobars that allows the existence of the mixed phase, irrespective of the particular form of the nuclear symmetry energy.

One should stress that different nuclear matter models, which fit the saturation point, display a rather diverse high density behavior of the nuclear symmetry energy. As mentioned already, variational calculations with phenomenological nucleon-nucleon potentials predict a density dependence that is incompatible with that of the RMF models. This discrepancy leads to serious uncertainty about some astrophysically relevant properties of the neutron star matter. Here we study the consequences of this uncertainty for the nucleon-quark phase transition in neutron star cores.

## II. QUARK MATTER IN NEUTRON STARS

Glendenning's construction describes a global division of the baryon number between two phases. It is insensitive to the geometrical form of the volume enclosing, respectively, nucleons and quarks. To account for the shape and size of droplets of each phase, one should include the surface tension at the interface between the nucleon matter and the quark matter, the Coulomb interaction, and the Debye screening. Inclusion of these effects results in some corrections to the equation of state, which do not alter considerably the results of this simple approach. We discuss finite-size effects in Sec. VI where both the Coulomb interaction and the surface tension are included in the calculations.

The equilibrium conditions, in the case where the geometry of droplets is neglected, are those for bulk systems. The neutron star matter is assumed to be  $\beta$  stable and charge neutral. Thermal effects are not expected to play any important role in neutron star cores. We neglect them and put the temperature  $T = 0$ .

The equilibrium conditions for the quark matter droplet to coexist with the nucleon medium are that pressure and chemical potentials in both phases coincide. We choose pressure as an independent variable. The coexistence requires that

$$\mu_N^n(p) = \mu_N^q(p) \quad (1)$$

and

$$\mu_P^n(p) = \mu_P^q(p), \quad (2)$$

where  $\mu_N^n$  and  $\mu_N^q$  are the neutron chemical potentials in the nucleon and the quark phase, respectively. Similarly,  $\mu_P^n$  and  $\mu_P^q$  are the proton chemical potentials in respective phases. To solve the above coexistence conditions we construct isobars for both phases of baryon matter.

The  $\beta$ -equilibrium condition reads

$$\mu_N^i - \mu_P^i = \mu_e, \quad i = n, q, \quad (3)$$

where  $\mu_e$  is the electron chemical potential, and  $n$  and  $q$  refer to the nucleon and the quark phases, respectively. It turns out that muons can safely be neglected as the electron chemical potential remains low. We assume that the electron distribution is uniform. In this case, neglecting the electron rest mass,

$$\mu_e = (3\pi^2 n_e)^{1/3}, \quad (4)$$

where  $n_e$  is the electron density.

Solutions of Eqs. (1) - (3) provide the densities of both baryon phases  $n_P$  and  $n_q$ , where  $n_P$  is the proton density and  $n_q$  is the electric charge density of quarks in units of  $e$ . The global charge neutrality condition requires that

$$V n_e = V_n n_P + V_q n_q, \quad (5)$$

where  $V_n$  is the volume occupied by nucleons and  $V_q$  is the volume of quarks. Since  $V_n + V_q = V$ , the total available volume, we can define a quantity  $\alpha = V_n/V$ , which is the fraction of space containing nucleons. The quarks occupy a complementary fraction,  $1 - \alpha$ , of the volume. From Eq. (5) we obtain  $\alpha$  in the form

$$\alpha = \frac{n_e - n_q}{n_P - n_q}. \quad (6)$$

At a sufficiently low pressure we expect  $\alpha = 1$ , as free quarks are absent in the neutron star matter. The first quark droplets form at some pressure  $p_i$ , which we refer to as the lower critical pressure. It corresponds to  $\alpha$  starting to deviate from unity for the first time. With increasing pressure, more space is filled with the quark matter and  $\alpha < 1$ . Nucleons disappear at the upper critical pressure  $p_f$ , with  $\alpha(p_f) = 0$ . For pressure in the range  $p_i < p < p_f$ , nucleon matter coexists with quark matter.

The lower and upper critical pressure values  $p_i$  and  $p_f$  depend on both the nucleon matter EOS and the model of the quark matter. In the next section we specify the quantities used in our calculations of properties of the mixed phase.

### III. THE NUCLEAR SYMMETRY ENERGY AT HIGH DENSITIES

Following Ref. [5], we adopt a simple parametrization of the nuclear matter EOS. As shown in Ref. [5], the results of variational many-body calculations with phenomenological nucleon-nucleon potentials can be simply parametrized as a function of the baryon number density and the proton fraction. The energy per particle can be expressed as

$$E(n, x) = T(n, x) + V_0(n) + (1 - 2x)^2 V_2(n), \quad (7)$$

where  $n$  is the baryon number density and  $x = n_P/n$  is the proton fraction. The kinetic energy contribution is

$$T(n, x) = \frac{3}{5} \frac{1}{2m} (3\pi^2 n)^{2/3} [(1 - x)^{5/3} + x^{5/3}]. \quad (8)$$

The functions  $V_0(n)$  and  $V_2(n)$  represent the interaction energy contributions. The form (7) of the energy per particle is a very good approximation of the numerical calculations as far as the  $x$  dependence is concerned [5].

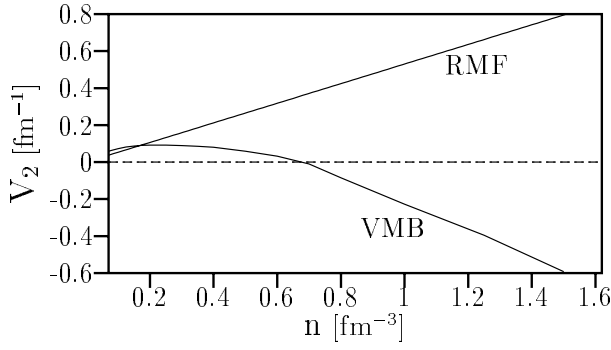


FIG. 1. The interaction energy  $V_2(n)$  as a function of the baryon number density, for the VMB and RMF models.

From Eq. (7) we obtain the pressure and chemical potentials of neutrons and protons. The pressure is

$$p = \frac{2}{5} \frac{1}{2m} (3\pi^2 n)^{2/3} n [(1-x)^{5/3} + x^{5/3}] + n^2 V'_0(n) + (1-2x)^2 n^2 V'_2(n). \quad (9)$$

The chemical potentials read

$$\begin{aligned} \mu_N^n = & \frac{1}{2m} (3\pi^2 n)^{2/3} [(1-x)^{5/3} + x(1-x)^{2/3}] + V_0(n) + nV'_0(n) \\ & + (1-4x^2)V_2(n) + (1-2x)^2 nV'_2(n) + m, \end{aligned} \quad (10)$$

$$\begin{aligned} \mu_P^n = & \frac{1}{2m} (3\pi^2 n)^{2/3} [x^{5/3} + (1-x)x^{2/3}] + V_0(n) + nV'_0(n) \\ & + (-3 + 8x - 4x^2)V_2(n) + (1-2x)^2 nV'_2(n) + m. \end{aligned} \quad (11)$$

Our aim here is to study the influence of the nuclear symmetry energy on the mixed phase properties. The energy per particle, Eq. (7), is well suited for this purpose as only the function  $V_2(n)$  enters the expression for the nuclear symmetry energy, which is

$$E_{sym}(n) = \frac{5}{9} T \left( n, \frac{1}{2} \right) + V_2(n). \quad (12)$$

To account for the uncertainty in high density behavior of  $E_{sym}(n)$ , we use different parametrizations of  $V_2(n)$ , keeping the function  $V_0(n)$  fixed.

As an example of variational many-body calculations, we use the EOS with the UV14+TNI interactions from Wiringa, Fiks, and Fabrocini [4]. Polynomial fits of this EOS are given in the Appendix. In Fig. 1 we show the function  $V_2(n)$  corresponding to the UV14+TNI interactions. One should note that with this  $V_2(n)$  the symmetry energy (12) reproduces the empirical value,  $E_{sym}(n_0) = 34 \pm 4$  MeV [6]. At higher densities,  $E_{sym}(n)$  saturates and then decreases, reaching negative values for  $n > 1.0$  fm<sup>-3</sup>.

The energy per particle of the RMF model can also be cast in the form (7) [7]. The function  $V_2(n)$  in this case is

$$V_2(n) = \frac{1}{8} \frac{g_\rho^2}{m_\rho^2} n. \quad (13)$$

The coupling parameter  $g_\rho^2/m_\rho^2$  is adjusted to fit the empirical value of the nuclear symmetry energy  $E_{sym}(n_0)$ . The function  $V_2(n)$ , Eq. (13), grows linearly with the baryon number density  $n$ , Fig. 1, and thus the nuclear symmetry energy in the RMF model increases monotonically with  $n$ . As we are concerned here mainly with the role of the symmetry energy, we model the energy per particle corresponding to the RMF theory using the function  $V_2(n)$  in the form (13) and keeping other contributions in Eq. (7) the same as in the VMB case.

The  $\beta$ -equilibrium condition (3) and the formulas (10) and (11) show that the proton fraction of the neutron star matter is fully determined by the function  $V_2(n)$ . In Fig. 2 we show the proton fraction corresponding to both forms of  $V_2(n)$ . For both curves, the proton fraction at  $n_0$  is  $x \approx 0.05$ . This is due to the empirical value  $E_{sym}(n_0)$ , which is

reproduced by both forms of  $V_2(n)$ . At higher densities, the behavior of  $x(n)$  is different in the two cases. The RMF model predicts that  $x(n)$  monotonically increases with the density, whereas for  $V_2(n)$  corresponding to the UV14+TNI interactions, the proton fraction decreases with  $n$ , and eventually protons disappear completely at some density  $n_v$ ,  $x(n_v) = 0$ . The disappearance of the proton fraction at high densities is a general property of nuclear interaction models that give  $V_2(n) < 0$  [8].

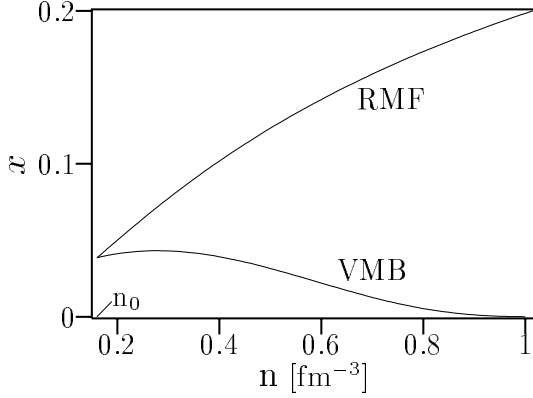


FIG. 2. The proton fraction of the  $\beta$ -stable neutron star matter corresponding to the interaction energy  $V_2(n)$  in Fig. 1, for VMB and RMF models.

#### IV. QUARK AND NUCLEON ISOBARS

The quark matter is described by a simple bag-model equation of state. We use the same parameters as in Ref. [2]. The energy density for three flavors is, neglecting bare masses,

$$\epsilon_q = \frac{3}{4}\pi^{2/3}(n_u^{4/3} + n_d^{4/3} + n_s^{4/3}) + B, \quad (14)$$

where  $n_i$ ,  $i = u, d, s$  are the quark number densities. The quark chemical potentials are

$$\mu_i = \pi^{2/3}n_i^{1/3}, \quad i = u, d, s. \quad (15)$$

The pressure of quark matter reads

$$p = \frac{1}{4\pi^2}(\mu_u^4 + \mu_d^4 + \mu_s^4) - B. \quad (16)$$

Below we show results corresponding to two values of the bag constant,  $B = 120$  MeV/fm<sup>3</sup> and  $B = 200$  MeV/fm<sup>3</sup>. We choose these values in order to assess the sensitivity of the mixed phase properties to the bag constant, which is treated here as a phenomenological parameter subject to a substantial uncertainty.

The  $\beta$  equilibrium requires that the chemical potential of down and strange flavors is the same,

$$\mu_d = \mu_s, \quad (17)$$

and the chemical potential of up quarks satisfies the condition

$$\mu_d = \mu_u + \mu_e. \quad (18)$$

Proton and neutron chemical potentials in the quark phase are

$$\mu_P^q = 2\mu_u + \mu_d, \quad (19)$$

$$\mu_N^q = \mu_u + 2\mu_d. \quad (20)$$

The simplest way to solve the equilibrium conditions (1) and (2) is to construct isobars for the nucleon and quark matter in the  $\mu_P - \mu_N$  plane. This can be done easily for the nucleon matter since proton and neutron chemical potentials, for a given value of pressure, are parametrized by one independent variable. For the quark phase, we impose the condition (17), which reduces the number of independent quark chemical potentials, for a given pressure, to two. Hence for each phase one can draw an isobar, a parametric curve in the  $\mu_P - \mu_N$  plane corresponding to a fixed pressure.

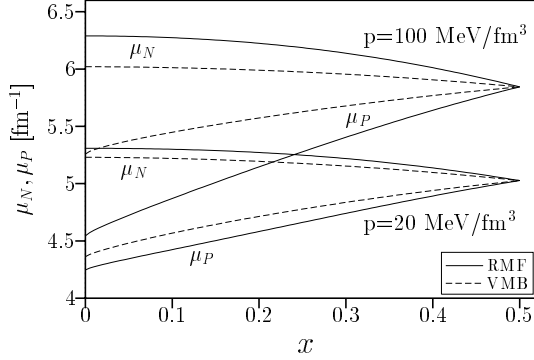


FIG. 3. Proton and neutron chemical potentials of nucleon matter as functions of the proton fraction for indicated values of pressure, for VMB and RMF models.

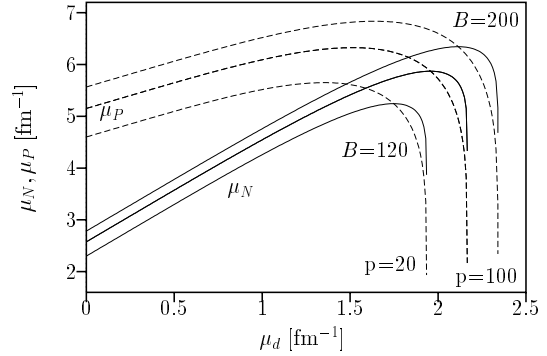


FIG. 4. Proton and neutron chemical potentials in quark matter as functions of the down-quark chemical potential. Values of pressure and the bag constant are in MeV/fm³. Solid and dashed curves correspond, respectively, to neutron and proton chemical potentials.

For the nucleon phase we parametrize isobars by the proton fraction  $x$ . As an example, in Fig. 3 we show proton and neutron chemical potentials as functions of  $x$  for two values of pressure,  $p = 20$  MeV/fm³ and  $p = 100$  MeV/fm³. One can see that for  $p = 20$  MeV/fm³ the proton and neutron chemical potentials corresponding to VMB and RMF models do not differ much from one another. For  $p = 100$  MeV/fm³, the VMB and RMF curves deviate significantly. In particular, the difference  $\mu_N(p, x = 0) - \mu_P(p, x = 0)$  decreases with pressure for the VMB model, whereas it increases for the RMF one.

In the quark phase, using the condition (17), one finds an isobaric relation between up and down quark chemical potentials in the form

$$\mu_u^4 = 4\pi^2(p + B) - 2\mu_d^4. \quad (21)$$

We choose  $\mu_d$  as an independent variable. In Fig. 4 the proton and neutron chemical potentials in the quark matter are shown for the same values of pressure as above,  $p = 20$  MeV/fm³ and  $p = 100$  MeV/fm³, for both values of the bag constant,  $B = 120$  MeV/fm³ and  $B = 200$  MeV/fm³. One can see that the curve corresponding to  $p = 20$  MeV/fm³ and  $B = 200$  MeV/fm³ coincides with that for  $p = 100$  MeV/fm³ and  $B = 120$  MeV/fm³.

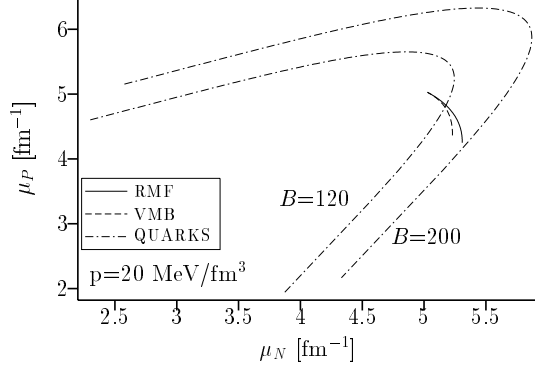


FIG. 5. VMB and RMF nucleon isobars, and quark isobars for two values of the bag constant, for pressure  $p = 20 \text{ MeV/fm}^3$ .

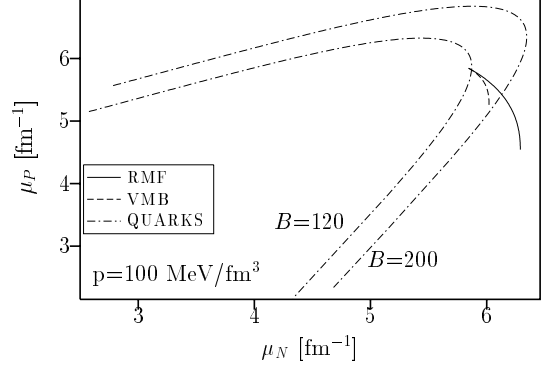


FIG. 6. The same as in Fig. 5 for pressure  $p = 100 \text{ MeV/fm}^3$ .

Isobars for the two phases are shown in Figs. 5 and 6, where  $\mu_P$  is plotted against  $\mu_N$  for  $p = 20 \text{ MeV/fm}^3$  and  $p = 100 \text{ MeV/fm}^3$ , respectively. The coexistence conditions (1) and (2) are fulfilled at the crossing point of the nucleon and quark isobars on the  $\mu_P - \mu_N$  plot. Also, the  $\beta$ -equilibrium condition (3) is satisfied at this point with the electron chemical potential  $\mu_e = \mu_P - \mu_N$ . This formula allows us to calculate the density of the homogeneous electron background  $n_e$  from Eq. (4).

The quark matter isobars are calculated assuming the strange quark mass to vanish,  $m_s = 0$ . This approximation is justified for pressure values relevant to our analysis, as in this range isobars corresponding to  $m_s = 0$  and to the empirical value of the strange quark mass,  $m_s = 150 \text{ MeV}$ , are similar. Also, the lowest values of the strange quark chemical potential obtained from the coexistence conditions (1) and (2),  $\mu_s \sim 400 \text{ MeV}$ , exceed the empirical mass  $m_s = 150 \text{ MeV}$  considerably. Corrections due to the empirical value of the strange quark mass would result in small changes of the critical parameters corresponding to the formation of the first quark droplets.

## V. RESULTS AND IMPLICATIONS FOR NEUTRON STARS

In order to find a critical pressure indicating the onset of the phase transition to quark matter, we analyze how the crossing of nucleon and quark isobars changes with pressure. For very low values of pressure,  $p \leq 1 \text{ MeV/fm}^3$ , the nucleon isobars for both VMB and RMF models do not cross the quark isobars, for both values of the bag constant. With increasing pressure, the lower end point of the nucleon isobar, corresponding to  $x = 0$ , merges with the quark isobar at some pressure value  $p_0$ . At this pressure pure neutron matter can coexist with quark matter. This, however, is not the situation encountered in neutron stars, where at this value of pressure the neutron star matter contains a small proton fraction of about 5%, as shown in Fig. 2. For higher pressure,  $p > p_0$ , the proton fraction at the crossing point of the nucleon isobar with the quark isobar increases. The formation of the first quark droplets in the nucleon medium starts at such a pressure  $p_i$  that the proton fraction of the nucleon matter at the crossing of the isobars coincides with that of the  $\beta$ -stable neutron star matter at this pressure. The pressure  $p_i$  is referred to as the lower critical pressure.

For  $B = 120 \text{ MeV/fm}^3$ , the lower critical pressure for the VMB and RMF isobars is, respectively,  $p_i = 2 \text{ MeV/fm}^3$  and  $p_i = 3 \text{ MeV/fm}^3$ . The upper critical pressure  $p_f$  at which the last nucleon droplets immersed in quark matter finally dissolve, is the same for both VMB and RMF isobars,  $p_f = 115 \text{ MeV/fm}^3$  (see Fig. 6).

In the case of  $B = 200 \text{ MeV/fm}^3$ , the lower critical pressure for VMB and RMF models is, respectively,  $p_i = 215 \text{ MeV/fm}^3$  and  $p_i = 35 \text{ MeV/fm}^3$ . The value of the upper critical pressure is  $p_f = 290 \text{ MeV/fm}^3$ .

The fraction of volume filled with nucleons,  $\alpha$ , is shown in Fig. 7. For the lower value of the bag constant,  $B = 120 \text{ MeV/fm}^3$ , the curves for VMB and RMF models are very similar. This is because the lower critical pressure  $p_i$  is almost identical in the two cases. The situation is quite different for  $B = 200 \text{ MeV/fm}^3$ . In this case the phase transition for the VMB model starts at much higher pressure than for the RMF model. This reflects the fact that the VMB isobar becomes much shorter at high pressure than the RMF one. One can easily see this difference in Fig. 6 where we show  $p = 100 \text{ MeV/fm}^3$  isobars.

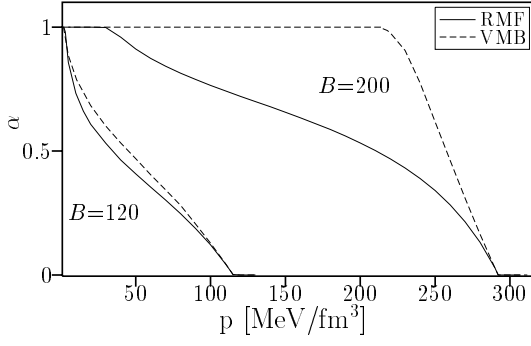


FIG. 7. The fraction of the mixed phase volume filled with nucleons as a function of pressure for VMB and RMF models and for both values of  $B$ .

The results shown in Fig. 7 prove that the properties of the nucleon-quark phase transition are very sensitive to the nuclear symmetry energy, for higher values of the bag constant. This is because, generally, the phase transition occurs at a higher pressure for higher values of the bag constant, and the VMB and RMF isobars differ much more at high values of pressure. For low values of  $B$ , the phase transition starts at a low enough pressure for the nuclear symmetry energy not to affect the isobars significantly.

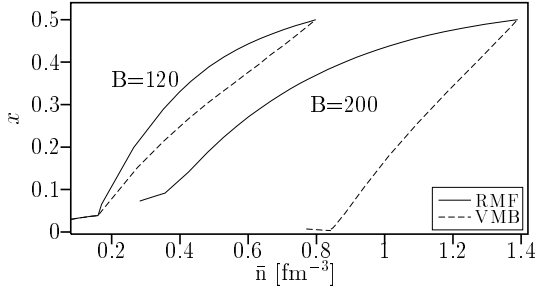


FIG. 8. The proton fraction of nucleon matter coexisting with quark matter as a function of the mean baryon number density.

In Fig. 8 we show the proton fraction of nucleon matter coexisting at a given pressure with quark matter, as a function of the mean baryon number density  $\bar{n}$ ,

$$\bar{n} = \alpha n + (1 - \alpha)n^Q, \quad (22)$$

where  $n$  and  $n^Q = (n_u + n_d + n_s)/3$  are the baryon number densities of, respectively, nucleon and quark matter. The density corresponding to the lower critical pressure  $p_i$  at which the phase transition starts is  $\bar{n}_i$ . The phase transition is completed at the density  $\bar{n}_f$  corresponding to the upper critical pressure  $p_f$ . For  $B = 120$  MeV/fm<sup>3</sup>,  $\bar{n}_i = 0.17$  fm<sup>-3</sup> is approximately the same for VMB and RMF models. One can notice that nucleon matter becomes more proton rich with increasing pressure irrespective of the nuclear symmetry energy. At the upper critical pressure  $p_f$  disappearing nucleon droplets for both nuclear models are composed of symmetric nuclear matter. The corresponding density is  $\bar{n}_f = 0.8$  fm<sup>-3</sup>. For  $B = 200$  MeV/fm<sup>3</sup> the quark droplets start to form at a density  $\bar{n}_i = 0.84$  fm<sup>-3</sup> and  $\bar{n}_i = 0.35$  fm<sup>-3</sup>, respectively, for the VMB and RMF models. Nucleons disappear at  $\bar{n}_f = 1.39$  fm<sup>-3</sup>.

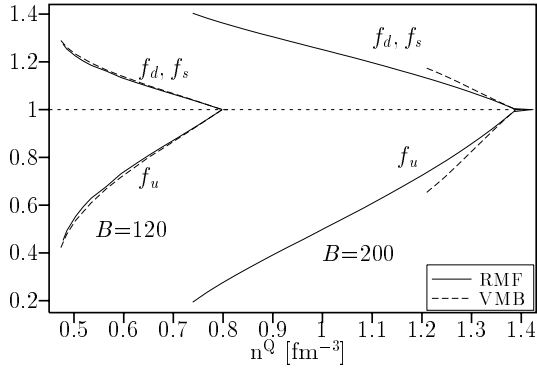


FIG. 9. Concentrations of quark flavors in quark matter coexisting with nucleon matter as functions of the quark baryon density.

Properties of quark matter in the mixed phase are displayed in Fig. 9, where the flavor composition is shown for both values of the bag constant. The flavor concentrations are  $f_i = n_i/n^Q$ ,  $i = u, d, s$ . A strong dependence of the mixed phase properties on the symmetry energy for  $B = 200$  MeV/fm<sup>3</sup> is best visible in this figure. Quark matter, forming the first droplets at the lower critical pressure  $p_i$ , is composed mostly of negatively charged quarks. With increasing pressure the flavor composition becomes more symmetric, and, at the upper critical pressure  $p_f$ , the concentrations of all flavors become equal,  $f_u = f_d = f_s$ . Quark matter at  $p \geq p_f$  is charge neutral.

The electron density is shown in Fig. 10. At the lower critical pressure  $p_i$ ,  $n_e = n_P$ , as only electrons compensate the positive charge carried by protons. With increasing pressure, negatively charged quarks become more abundant and the electron density decreases. Electrons disappear at the pressure  $p_f$  when the whole available volume is filled with electrically neutral quark matter.

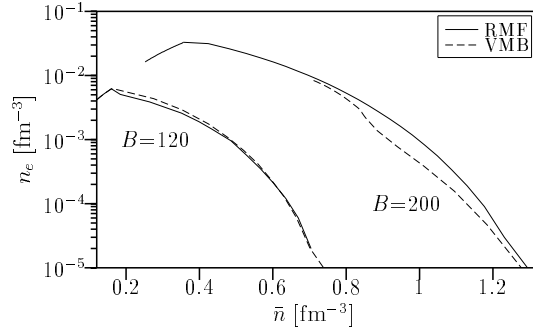


FIG. 10. The electron density of the uniform electron background as a function of the mean baryon number density.

To investigate the consequences of the existence of a mixed quark-nucleon phase for neutron stars we construct the equation of state  $p = p(\bar{\rho})$ , where the mass density of the mixed phase is

$$\bar{\rho} = \frac{1}{c^2} [\alpha \epsilon_{nuc} + (1 - \alpha) \epsilon_q]. \quad (23)$$

In Fig. 11 masses of neutron stars are shown as functions of the central density for pure nucleon matter and for the mixed quark-nucleon phase. The phase transition to quark matter makes the equation of state softer. The maximum mass of neutron stars containing the mixed phase decreases as compared with the pure nucleon case. The effect is stronger for low values of the bag constant, as the mixed phase comprises more mass of the star than for higher  $B$ . Results shown in Fig. 11 exclude, in fact, low values of the bag constant, as for  $B \leq 120$  MeV/fm<sup>3</sup> the maximum mass is below the observational limit. For  $B = 200$  MeV/fm<sup>3</sup> the maximum mass safely exceeds this limit. In this case, the influence of the nuclear symmetry energy is clearly visible. The maximum mass corresponding to the RMF model is well below that for the VMB model. Generally, reduction of the maximum mass due to the presence of



the mixed phase is much more significant for the RMF model than for the VMB one. This reflects the fact that for  $B = 200 \text{ MeV/fm}^3$  the phase transition to quark matter starts at much lower pressure in the RMF model than in the

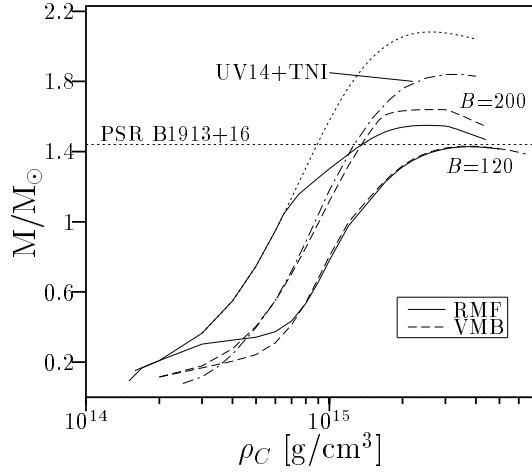


FIG. 11. Neutron star masses as functions of the central density. The dotted line corresponds to pure nucleon matter in the RMF model. The dash-dotted line is for pure nucleon VMB equation of state. Solid and dashed curves are for equations of state involving the mixed quark-nucleon phase. The horizontal line shows the empirical lower limit to the maximum neutron star mass.

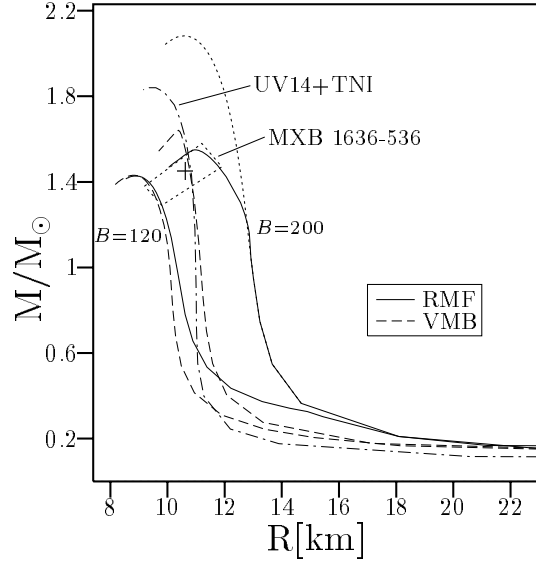


FIG. 12. Neutron star masses as functions of the radius for the same equations of state as in Fig. 11. The cross and the error box represent empirical constraints for the x-ray source MXB 1636-536.

VMB case. Correspondingly, the mixed phase core of the maximum mass neutron star is much smaller for the VMB model than for the RMF one.

We also show in Fig. 12 neutron star masses as functions of the radius for the same EOS's as in Fig. 11. The error box indicates the constraints on the mass-radius relation for the x-ray burst source MXB 1636-536. In this case, equations of state involving a mixed phase with the bag constant  $B = 120 \text{ MeV/fm}^3$  are marginally compatible with the data.

It is interesting to note that the structure of a neutron star of the canonical mass  $M = 1.44M_\odot$  is even more sensitive to the form of the nuclear symmetry energy. For  $B = 200 \text{ MeV/fm}^3$ , with the RMF symmetry energy, such a star, whose radius is  $\sim 12 \text{ km}$ , possesses a mixed phase core of  $\sim 7 \text{ km}$  radius. In the VMB model, the star is composed entirely of nucleons. The central pressure of the VMB star,  $p_c = 120 \text{ MeV/fm}^3$ , is below the lower critical value  $p_i = 215 \text{ MeV/fm}^3$  at which the phase transition to the mixed quark-nucleon matter begins.

## VI. COULOMB AND SURFACE EFFECTS

Up to now we did not consider the space structure of the mixed phase. When the Coulomb interaction and the surface tension are included in the calculations, one can find a variety of geometric structures formed by regions filled with nucleons and quarks that have opposite electric charge density [9]. The form of these structures changes with the fraction of space filled with nucleons,  $\alpha$ . It should be stressed, however, that the mixed phase (called also, following Ref. [2], the droplet phase) is the ground state of the neutron star matter only if the surface tension at the interface between nucleon and quark matter remains sufficiently small [2]. In the opposite case, the mixed phase will not be favored energetically and a phase transition will lead to the coexistence of two bulk electrically neutral phases. We investigate here how the high density behavior of the nuclear symmetry energy influences the Coulomb and surface effects in the droplet phase.

We perform calculations using the Wigner-Seitz approximation. In this approach we assume that characteristic sizes of structures in the droplet phase are less than the Debye screening length, which is about 10 fm for the nucleon phase and 5 fm for quarks [2]. In this case electrons are essentially uniformly distributed over the whole system and so are other particles within a given phase. When the spatial scale of structures is larger than the screening length the charge density becomes nonuniform and the mixed phase resembles two coexisting neutral phases.

The geometric forms of structures considered here are droplets or bubbles, rods, plates, and also intermediate forms, each of them characterized by a continuous dimensionality parameter  $d$  ranging from  $d = 3$  for droplets to  $d = 1$  for plates. For all these geometries the minimized sum of Coulomb and surface energy densities reads

$$\epsilon_C + \epsilon_\sigma = 6\pi\chi \left( \frac{\sigma^2 d^2 [n_P(\alpha) - n_q(\alpha)]^2 e^2 f_d(\chi)}{16\pi^2} \right)^{1/3}. \quad (24)$$

The radius of the rare phase bubble immersed in the dominant phase is

$$r = \left( 4\pi \frac{[n_P(\alpha) - n_q(\alpha)]^2 e^2 f_d(\chi)}{\sigma d} \right)^{-1/3}. \quad (25)$$

Here  $n_P(\alpha)$  and  $n_q(\alpha)$  are charge densities of nucleons and quarks, in units of  $e$ , corresponding to a given proportion of phases  $\alpha$ . The quantity  $r$  expresses the characteristic sizes of geometric forms and particularly for droplets and rods is their radius, and in the case of plates is their half thickness. In the above equations  $\chi$  is the fraction of volume occupied by the rare phase. It is equal to  $1 - \alpha$  when nucleons are the dominant phase ( $\alpha \geq 1/2$ ) and quarks form different structures, and it is simply  $\alpha$  in the opposite situation ( $\alpha \leq 1/2$ ). It also defines the half distance between structures,  $R$ , which is the radius of the Wigner-Seitz cell. The fraction  $\chi$  can be expressed in terms of the two scales  $r$  and  $R$  as

$$\chi = (r/R)^d. \quad (26)$$

The function  $f_d(\chi)$  is

$$f_d(\chi) = \frac{1}{d+2} \left( \frac{1}{d-2} \left( 2 - d\chi^{1-2/d} \right) + \chi \right). \quad (27)$$

It has a correct logarithmic limit for  $d = 2$ .

Having the values of  $n_P$  and  $n_q$  from Eqs. (1)-(3), and (5) we are able to calculate finite-size effects in the quark-nucleon mixed phase. The values of both  $\epsilon_C + \epsilon_\sigma$  and  $r$  are obtained by minimization of the energy, Eq. (24), with

respect to  $d$  for a given proportion of phases  $\alpha$  and for fixed  $\sigma$ . Because the exact value of the surface tension is unknown we keep it as in the work of Heiselberg *et al.* [2] as a parameter which for simplicity is density independent.

For the mixed phase to be favorable, its energy density must be less than the energy densities of all other phases of baryon matter. When  $\sigma = 0$  and Coulomb and surface effects are absent the mixed phase is energetically favored, as we showed in Sec. IV by performing a proper construction of the phase transition. Nevertheless, when  $\sigma \neq 0$  the situation is different and for some high values of the surface tension the mixed phase becomes energetically unfavorable. Therefore to see what is the ground state of neutron star matter one should compare the energy density of the droplet phase with the energy densities of nucleon matter, quark matter, and coexisting electrically neutral phases of nucleon and quark matter.

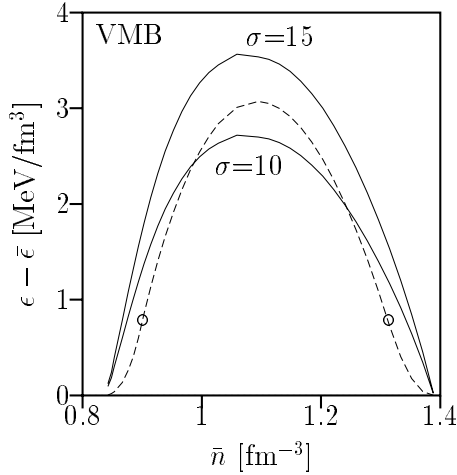


FIG. 13. The energy density of the mixed phase in the VMB model, for indicated values of surface tension  $\sigma$  (in  $\text{MeV}/\text{fm}^2$ ), relative to its value for  $\sigma = 0$  (solid curves). The dashed curve is the energy gain in the mixed phase with  $\sigma = 0$ , with respect to electrically neutral nucleon matter, quark matter and coexisting phases of nucleon and quark matter. Open circles correspond to bulk neutral nucleon matter and quark matter that can coexist in the first order phase transition.

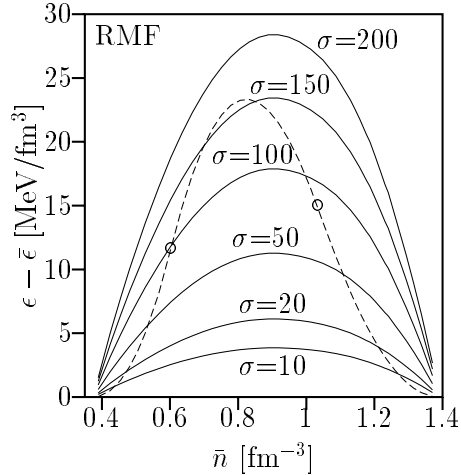


FIG. 14. The same as in Fig. 13 for the RMF model.

To account for the energy density of coexisting phases of electrically neutral nucleon matter and quark matter we perform a double-tangent construction of the phase transition from nucleon to quark matter. The energy density gain in the mixed phase with respect to nucleon matter, quark matter, and coexisting neutral phases of nucleon and quark matter,  $\epsilon - \bar{\epsilon}$ , where  $\bar{\epsilon}$  is the energy density of the mixed phase for  $\sigma = 0$ , is shown as a dashed curve in Fig. 13 and Fig. 14 for VMB and RMF models, respectively.

We show here results only for the bag constant  $B = 200 \text{ MeV}/\text{fm}^3$  as possibly realized in nature. As one sees, the difference in energy densities is strongly dependent on the nuclear symmetry energy. For the VMB model it is only a few  $\text{MeV}/\text{fm}^3$  whereas it is almost  $25 \text{ MeV}/\text{fm}^3$  for the RMF model. This implies that the allowed range of finite-size effects for the droplet phase to be energetically favorable will be smaller in the former case and larger in the latter. In Figs. 13 and 14 the solid curves represent the contributions of Coulomb and surface effects to the energy density of the droplet phase, for the indicated values of the surface tension. If the solid curve for a given  $\sigma$  lies below the dashed one in some range of the baryon number density  $\bar{n}$ , then the droplet phase will be the ground state of neutron star matter. If not, the droplet phase will not be preferred energetically and transition between two electrically neutral phases will occur. As is shown, our results yield  $\sigma \leq 10 \text{ MeV}/\text{fm}^2$  for the VMB model and  $\sigma \leq 150 \text{ MeV}/\text{fm}^2$  for the RMF one. We can thus conclude that the appearance of the mixed phase, although dependent on the exact value of the surface tension, is also very sensitive to the form of the nuclear symmetry energy.

The above calculations were made neglecting the Debye screening, which is justified for small size of the structures. In Fig. 15 and Fig. 16 we show typical diameters of bubbles and their separations for the VMB and RMF model,

respectively. As one sees in Figs. 15 and 16, for higher values of the surface tension the characteristic sizes of structures

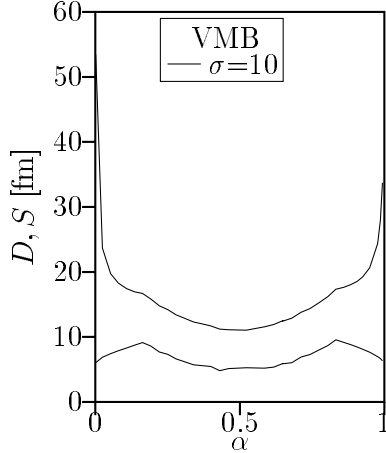


FIG. 15. Diameter (lower curve) and separation (upper curve) of structures in the mixed phase for the VMB model. The surface tension is  $\sigma = 10$  MeV/fm<sup>2</sup>.

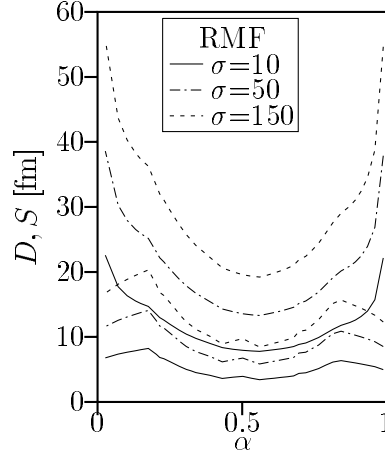


FIG. 16. The same as in Fig. 15 for the RMF model and for  $\sigma = 10, 50$ , and  $150$  MeV/fm<sup>2</sup>.

are larger than screening lengths in nucleon and quark matter so that the assumption of uniform charge distribution may not be valid.

## VII. DISCUSSION

We have studied the formation of a mixed quark-nucleon phase in neutron stars, for different models of the nuclear symmetry energy. We conclude that the behavior of nucleon matter isobars in the  $\mu_P - \mu_N$  plane, as, e.g., in Figs. 5 and 6, is fully responsible for the existence of the mixed phase. The isobars, for any pressure, have a common end point, corresponding to  $x = 1/2$ , which is thus independent of the nuclear symmetry energy. For  $x < 1/2$  the isobars corresponding to various forms of the nuclear symmetry energy differ considerably. The most different is the location of the  $x = 0$  end point of isobars (see Figs. 5 and 6).

The lower critical pressure  $p_i$  for the first quark droplets to form is determined by the location of the  $x = 0$  end point of a nucleon isobar, which strongly depends on the form of the nuclear symmetry energy. The upper critical pressure  $p_f$  for the last nucleons to dissolve into quarks is the same for all isobars that differ only in the form of the function  $V_2(n)$  determining the nuclear symmetry energy. This explains why nucleon matter coexisting with quark matter becomes proton rich with increasing pressure, and disappearing nucleon matter at the critical pressure  $p_f$  is symmetric. In Ref. [1] the increase of the proton fraction of nucleon matter coexisting in the mixed phase was attributed to the particular form of the nuclear symmetry energy in the RMF model.

Properties of neutron stars depend on both lower and upper critical pressure values,  $p_i$  and  $p_f$ . Since the lower critical pressure  $p_i$  strongly depends on the nuclear symmetry energy, properties of neutron stars also depend on it. In particular, the size of the mixed phase core, which determines the maximum mass of a neutron star, is rather sensitive to the nuclear symmetry energy. Conclusions concerning the presence of the mixed quark-nucleon phase in neutron stars are thus subject to some uncertainty that reflects incompatible high density predictions of the nuclear symmetry energy.

When the Coulomb interaction and the surface tension are included in the calculations, one can determine the surface tension values for which the mixed quark-nucleon phase is the ground state of neutron star matter. As shown in Fig. 13 and Fig. 14 the allowed range of  $\sigma$  is very narrow for the VMB model ( $\sigma < 10$  MeV/fm<sup>2</sup>), whereas it is much wider for the RMF model ( $\sigma < 150$  MeV/fm<sup>2</sup>).

## ACKNOWLEDGMENT

This research was partially supported by the Polish State Committee for Scientific Research (KBN), under Grant No. 2 P03B 112 17.

## APPENDIX

We fit the interaction energies  $V_0(n)$  and  $V_2(n)$  from Ref. [4] corresponding to the UV14+TNI interactions with the following polynomials:

$$V_0(n) = -0.0827n^4 - 0.3111n^3 + 2.2624n^2 - 1.181n - 0.0571 \quad (\text{A1})$$

and

$$V_2(n) = 0.0528n^4 + 0.1n^3 - 0.836n^2 + 0.433n + 0.0365. \quad (\text{A2})$$

Values of both functions are in  $\text{fm}^{-1}$ .

---

- [1] N. K. Glendenning, Phys. Rev. D **46**, 1274 (1992).
- [2] H. Heiselberg and C. J. Pethick, E. F. Staubo, Phys. Rev. Lett. **70**, 1355 (1993).
- [3] B. D. Serot and H. Uechi, Ann. Phys. (N.Y.) **179**, 272 (1987).
- [4] R. B. Wiringa, V. Fiks, and A. Fabrocini, Phys. Rev. C **38**, 1010 (1988).
- [5] I. E. Lagaris and V. R. Pandharipande, Nucl. Phys. **A369**, 470 (1981).
- [6] W. D. Myers, At. Data Nucl. Data Tables **17**, 411 (1976); H. v. Groote, E. R. Hilf, and K. Takahashi, *ibid.* **17**, 418 (1976); P. A. Seeger and W. M. Howard, *ibid.* **17**, 428 (1976); M. Bauer, *ibid.* **17**, 442 (1976); J. Jänecke and B. P. Eynon, *ibid.* **17**, 467 (1976);
- [7] M. Kutschera, Z. Phys. A **348**, 263 (1994).
- [8] M. Kutschera, Acta Phys. Pol. B **29**, 25 (1998).
- [9] D. G. Ravenhall, C. J. Pethick, and J. R. Wilson, Phys. Rev. Lett. **50**, 2066 (1983).